19 February 2002

Chemical Physics Letters 353 (2002) 295–303

CHEMICAL PHYSICS LETTERS

www.elsevier.com/locate/cplett

Dissociative ionization of halogenated ethylenes in intense femtosecond laser pulses

Marta Castillejo [a,*], Margarita Martín [a], Rebeca de Nalda [a,1], Stelios Couris [b,2], Emmanuel Koudoumas [b]

[a] *Instituto de Química Física "Rocasolano", CSIC, Serrano 119, 28006 Madrid, Spain*
[b] *Institute of Electronic Structure and Laser, Foundation for Research and Technology, Hellas, P.O. Box 1527, 711 10 Heraklion, Crete, Greece*

Received 19 November 2001; in final form 2 January 2002

Abstract

The interaction of chloro-ethylene ($H_2C{=}CHCl$), bromo-ethylene ($H_2C{=}CHBr$), and 2-chloro-ethenylsilane ($H_3SiCH{=}CHCl$) with 50 fs linearly polarized laser pulses of 800 and 400 nm at intensities up to 2×10^{14} and 7×10^{12} W cm^{-2}, respectively, has been studied using a time-of-flight mass spectrometer. At 400 nm extensive fragmentation is observed, while at 800 nm the presence of singly and doubly charged parent ions and of multiply charged atomic ions in the mass spectra attests to a reduction of fragmentation in favour of multiple ionization of the parent followed by Coulomb explosion. The silane compound dissociates more easily, its multicharged atomic fragments appear at lower intensities and are ejected with higher kinetic energies than the chlorine and bromine derivatives. The results reveal that laser–molecule coupling is influenced by the molecular properties and that energy channeling increases with molecular size.

1. Introduction

The dissociative ionization of polyatomic molecules following the interaction with intense laser fields has lately attracted a great deal of attention [1–8]. Successive multiple electron removal from the parent molecule is followed by dissociation into molecular and atomic fragments. Multiply charged fragments are produced by multiply ionized precursors that undergo Coulomb explosion. Dissociative ionization is relevant for the understanding of other processes that take place under strong laser excitation such as anisotropic fragment ejection [9,10], molecular alignment [11–13], high harmonic generation [14,15] and coherent control [16]. An important subject of research is the relevance of the molecular structure to the proper description of the processes involved [1,17–19]. If the laser–molecule coupling is sensitive to the intramolecular dynamics, molecular properties would have to be

* Corresponding author. Fax: +34-91-564-2431.
E-mail address: marta.castillejo@iqfr.csic.es (M. Castillejo).
[1] Present address: The Blackett Laboratory, Imperial College of Science, Technology and Medicine, London SW7 2BW, UK.
[2] Present address: ICEHT-FoRTH, P.O. Box 1414, 26500 Patras, Greece.

0009-2614/02/$ - see front matter
PII: S0009-2614(02)00039-8

invoked as opposed to the interaction with a mere set of independent atoms.

Here we report a study of the interaction of 50 fs laser pulses with wavelengths of 800 and 400 nm, at intensities up to 2×10^{14} and 7×10^{12} W cm^{-2}, respectively, with the ethylene derivatives chloro-ethylene (H_2C=CHCl), bromo-ethylene (H_2C=CHBr), and 2-chloro-ethenylsilane (H_3Si CH=CHCl). Laser-induced ionization and dissociation of these molecules has been investigated using time-of-flight mass (TOF) spectrometry. Another work [20] has presented our studies on the anisotropic distributions of ion fragments obtained at 800 nm and a brief account of the TOF spectra obtained at this wavelength. In the present Letter we will focus on the mechanisms leading to the observed fragment distributions and peak splitting and their dependence on laser intensity and wavelength, and the molecular structure and properties. Chloro- and bromo-ethylene are planar systems, whereas in 2-chloro-ethenylsilane the Si—H bonds lie outside the molecular plane. 2-Chloro-ethenylsilane also features the largest geometrical size of the three systems. The highly electronegative halide substituents confer a high polarizability to these molecules. The average electric dipole polarizability of chloro- and bromo-ethylene is 6.41×10^{-24} and 7.59×10^{-24} cm^3, respectively [21]. The estimated value of 2-chloro-ethenylsilane, using standard bond distances and angles [21], is 11.0×10^{-24} cm^3.

2. Experimental

The experimental technique, including the laser system, has been described elsewhere [8,20] and therefore only a short overview is given here. The laser system is an amplified Ti:Sapphire laser consisting of a Mira Ti:Sapphire oscillator (coherent) and a BMI regenerative Ti:Sapphire amplifier. The laser delivers pulses at 800 nm with a linewidth of about 40 nm at a repetition rate of 1 kHz. The pulse width was measured to be 50 fs by using a home-made autocorrelator.

The linearly polarized laser beam at 800 nm was focused with a 15 cm lens at the center of the extraction region of a time-of-flight (TOF) mass spectrometer. Special care was taken in order to ensure that no space–charge effects were perturbing the mass spectral measurements. The pulse energy could be continuously varied in the range 8–500 μJ by means of Glan polarizers and was measured at the exit of the chamber with an energy meter (Molectron J3-09). In order to check for possible nonlinear effects caused by the Glan polarizers, we carried out additional measurements in which the laser intensity was controlled by means of variable neutral-density filters; no significant alterations of the mass spectra were thus found. The B-integral [22] of the optical setup was calculated to be 1.2 and 0.06 for the maximum intensities of the 800 and 400 nm beams, respectively. As these values are well below the accepted critical limit of 3–5, the role of nonlinear effects induced by the optical elements and windows of the vacuum chamber should have a negligible influence. Additionally, we checked the spectrum, the duration and the polarization of the laser pulse after the passage through the TOF chamber to make sure that there was no effect of the experimental setup on the laser beam. The intensities of the laser were calibrated by measuring the saturation intensity for the ionization of Xe [23,24]. At 800 nm the available intensities range between 3×10^{12} and 2×10^{14} W cm^{-2}. Laser pulses at 400 nm were produced by second-harmonic generation in a BBO crystal. After focusing in the interaction region, intensities up to 7×10^{12} W cm^{-2} were available at the second-harmonic wavelength. The polarization of the laser light, defined by the Glan polarizer, could be rotated using a half wave plate. The angle between the detection axis of the TOF and the polarization vector of the laser defined the polarization angle. The laser was polarized along the TOF axis in *p*-polarization.

The mass spectra were measured with a linear TOF spectrometer. The photo-ions generated in the ionization and fragmentation processes were accelerated between a repeller plate (+1900 V) and a grounded electrode 1.5 cm apart, passed into a 60 cm long TOF tube, and detected and amplified with a pair of microchannel plates (MCP) of a 2.54 cm diameter. The MCP signals were fed into a

LeCroy 9414 digital oscilloscope, interfaced with a PC. The mass spectra were typically averaged over 200 laser shots.

Samples of the pure molecular compounds or in mixtures with Helium were expanded from stagnation pressures between 20 and 300 Torr into the vacuum chamber through a 0.3 mm pulsed nozzle (Laser Technics). The laser interaction zone is about 2 cm downstream from the nozzle. The molecules are cooled to an estimated rotational temperature of about 40–50 K as measured using CO as reference gas. Chloro-ethylene and bromo-ethylene were purified by trap-to-trap distillation. 2-Chloro-ethenylsilane was synthesized [25] as a 1:3 mixture of *cis* and *trans* isomers. These compounds were 95% pure as found by gas chromatography.

3. Results

3.1. Mass spectra

The TOF spectra of the three molecules under study were recorded as a function of laser intensity. At 800 nm the intensities were in the 3×10^{12}–2×10^{14} W cm^{-2} range and at the second harmonic, 400 nm, in the 1.5×10^{12}–7×10^{12} W cm^{-2}

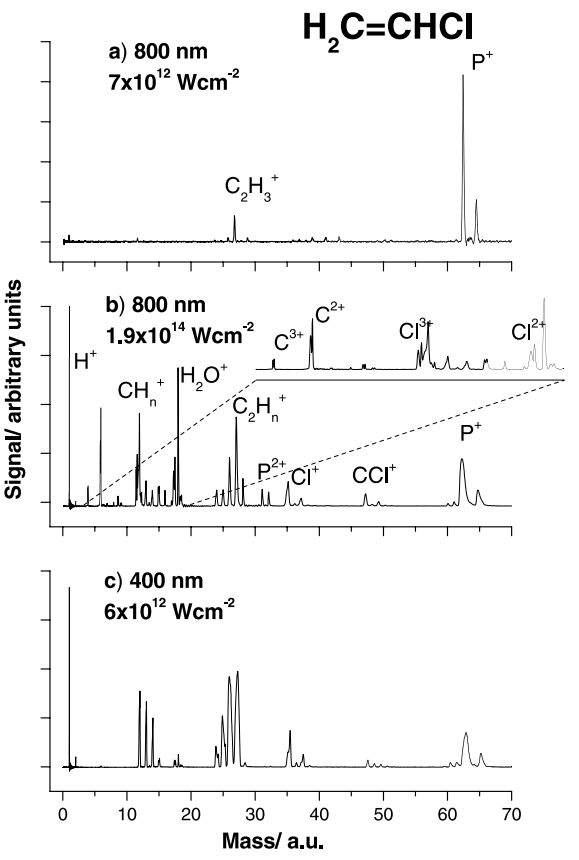

Fig. 1. TOF spectra of chloro-ethylene (stagnation pressure of pure compound 20 Torr) recorded at: (a) 800 nm, 7×10^{12} W cm^{-2}; (b) 800 nm, 1.9×10^{14} W cm^{-2}; (c) 400 nm, 6×10^{12} W cm^{-2}. P^+ indicates the parent ion. The inset illustrates the typical double peak structure of the multiply charged ions observed in this work.

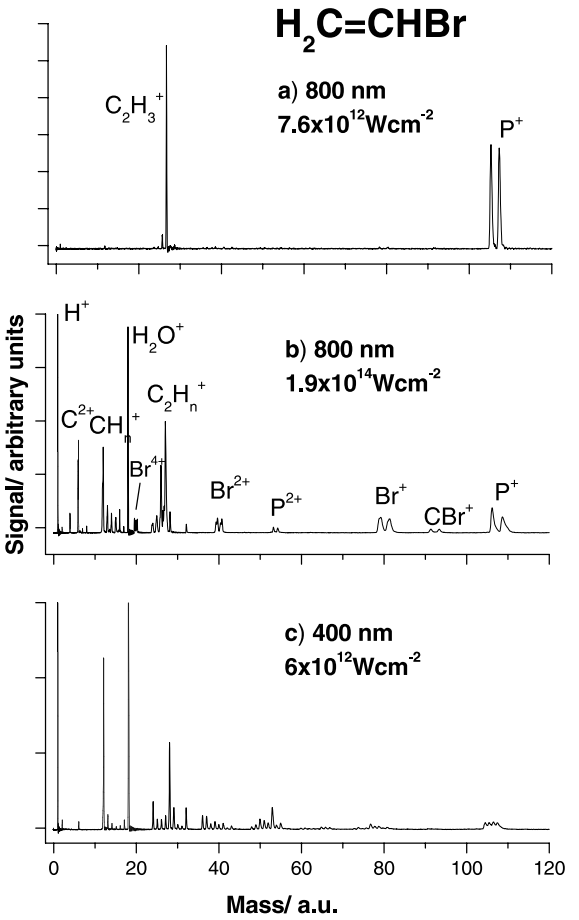

Fig. 2. TOF spectra of bromo-ethylene (stagnation pressure of pure compound 20 Torr) recorded at: (a) 800 nm, 7.6×10^{12} W cm^{-2}; (b) 800 nm, 1.9×10^{14} W cm^{-2}; (c) 400 nm, 6×10^{12} W cm^{-2}. P^+ indicates the parent ion.

range. The dependence on laser intensity of the parent and the fragment ion yields and the observed peak splittings could thus be studied.

Figs. 1–3 show mass spectra of the three ethylene derivatives obtained under several laser conditions and stagnation pressure of pure compound around 20 Torr. For chloro-ethylene, the spectra recorded at low intensity of the fundamental radiation at 800 nm (Fig. 1a) contain contributions of the parent and the $C_2H_3^+$ fragment ions only. As the laser intensity rises (Fig. 2b) other peaks appear: (a) the singly charged atomic and molecular fragments $H^+, C^+, Cl^+, CCl^+, CH_m^+$ $(m = 1$ to $3)$ and $C_2H_n^+$ $(n =$ 0 to 2), (b) the parent dication and (c) the multiply charged C and Cl atomic ions with up to 3 and 4 positive charges, respectively. The parent ion peak is observed to broaden as the laser intensity increases due to the enlargement of the interaction region in which the laser intensity overcomes the onset for ionization. At 400 nm (Fig. 1c) the parent ion peak is very weak even at the lowest intensities, indicating that extensive fragmentation occurs at this wavelength in the intensity range explored here; C^{2+} and Cl^{2+} are present at 6×10^{12} W cm^{-2}. Bromo-ethylene behaves similarly to the chlorine derivative. The $C_2H_3^+$ fragment is predominant at low intensities of the laser at 800 nm (Fig. 2a) whereas more fragmentation and appreciable contributions from the parent dication and multicharged atomic C and Br ions is evident at higher intensities (Fig. 2b). At 400 nm fragmentation (Fig. 2c) is almost complete; C^{2+} is the only multicharged ion observed. The TOF spectra of 2-chloro-ethenylsilane (Fig. 3) are somewhat more complex than the spectra corresponding to chloro- and bromo-ethylene. The spectra shows signs of a high degree of fragmentation at both wavelengths even for low incident intensities, probably reflecting the larger number of available dissociation channels. $C_nH_m^+, SiC^+, CCl^+$, and ions containing the SiC_2 and SiCl skeletons are observed. At 800 nm the parent dication and the multiply charged C, Cl and Si ion peaks (with charges up to 3, 5 and 4, respectively) contribute appreciably to the spectrum but are not present at 400 nm (only C_2^+ is observed at this wavelength).

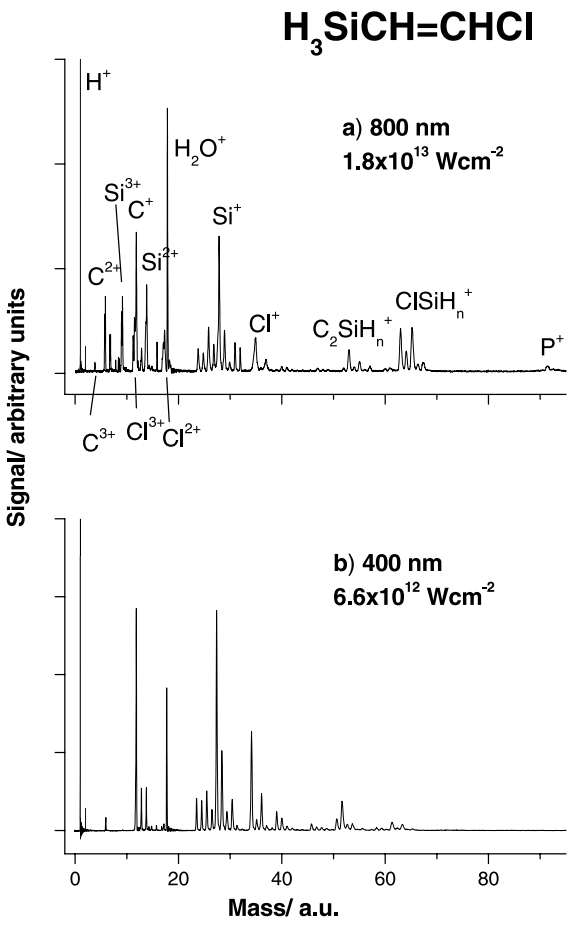

Fig. 3. TOF spectra of 2-chloro-ethenylsilane (stagnation pressure of pure compound 20 Torr) recorded at: (a) 800 nm, 1.8×10^{13} W cm^{-2}; (b) 400 nm, 6.6×10^{12} W cm^{-2}. P^+ indicates the parent ion.

In the three systems all the halogen-containing ions appear as a double-peak structure with relative intensities consistent with the isotopic abundance ratios. Background signals due to hydrogen, oxygen, nitrogen and particularly water are also present. The coincidence of mass to charge ratio of some of the multiply charged atomic fragment ions from the studied molecules and the background gases, i.e., N^{2+} and Cl^{5+} or N^+ and Si^{2+}, could complicate the analysis of the spectra. However the characteristic isotopic splitting helps to elucidate the provenance of the ions. The effects of clustering in the TOF spectra are likely to be

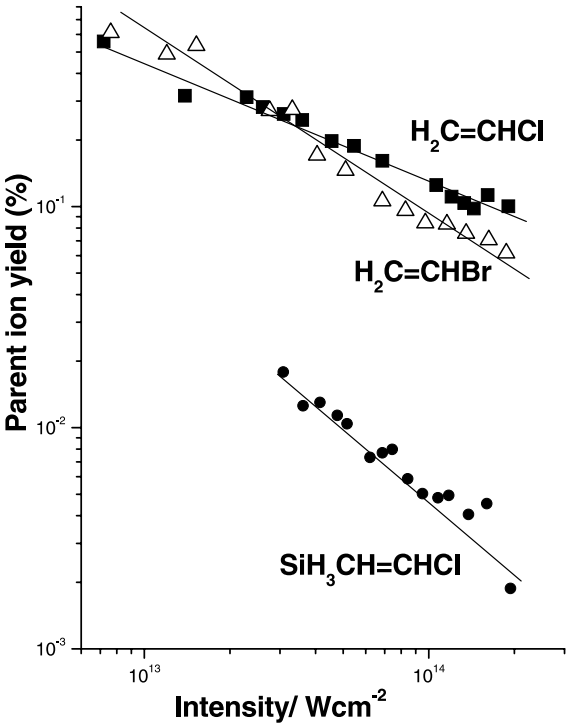

Fig. 4. Parent ion yield (summed areas of the parent ion peaks, P^+ and P^{2+}, versus the total area of the TOF spectrum) as a function of laser intensity at 800 nm. Squares, triangles and circles represent chloro-ethylene, bromo-ethylene and 2-chloro-ethenylsilane respectively. The straight lines are visual guides.

negligible. We found, moreover, that enhancing the stagnation pressure up to 760 Torr with the addition of He did not affect significantly the mass spectra of the studied molecules.

At a given laser intensity the ion distribution was found to be dependent on laser wavelength. At 6×10^{12} W cm^{-2} and laser wavelength of 400 nm, the $C_2H_3^+$ signal is around two times more intense than that of the chloro-ethylene parent ion peak. At 800 nm and similar laser intensity, the parent ion signal is eight times more intense than the fragment signal. However, at this wavelength, the predominance of the parent ion peak is only observed below 2×10^{13} W cm^{-2}; at higher intensities the ion yields approach a saturation regime in which the $C_2H_3^+$ signal is around two times that of the parent ion. In bromo-ethylene the $C_2H_3^+$ signal is similar at 800 nm and much more intense at 400 nm to that of the parent ion. In 2-chloro-ethenylsilane the $C_2H_3^+$ peak is always more intense that the parent ion peak regardless of the intensity and wavelength. These results indicate a tendency to more extensive dissociation as the molecular weight and size increases.

The relative contribution of the parent ion to the total ionization signal gives an indication of the stability of the molecular ion against fragmentation. Fig. 4 shows how the relative parent ion yield depends on laser intensity at 800 nm. One can see that the parent molecular ions of both chloro- and bromo-ethylene can sustain, without bond breaking, higher laser intensities than 2-chloro-ethenylsilane, a molecule with bigger size both in number of atoms and in geometrical dimensions. This must be related with the higher number of fragmentation channels open for the latter. The fact that fragmentation is greater when the size of the molecule increases indicates that efficient coupling of laser energy into the nuclear degrees of freedom is taking place. Similar scaling with molecular size has been observed in other polyatomic systems [1,19].

The evolution with laser intensity of the multiply charged atomic ion provides information about the interaction taking place in the highest intensity spatial and temporal regions of the laser pulse. As an example we show in Fig. 5 a log–log plot of the dependence of C^{n+}, Si^{n+} and Cl^{n+} signals from 2-chloro-ethenylsilane on laser intensity. An initial rapid rise with intensity is observed in all cases. Saturation of the process causes the slope to decrease as the onset for the appearance of the higher charge ions is reached. At intensities below saturation, the slope is higher for the ions with higher charge multiplicity. It has been observed that the onset for the apparition of multiply charged halogen ions in 2-chloro-ethenylsilane is lower than the corresponding onset for ions from chloro- and bromo-ethylene. Thus, the explosion of the parent molecule to produce multicharged atomic fragments occurs at lower intensities in the silane compound. This fact provides one more evidence that laser energy is more efficiently channelled into the silane derivative than into the chloro- and bromo-ethylene systems.

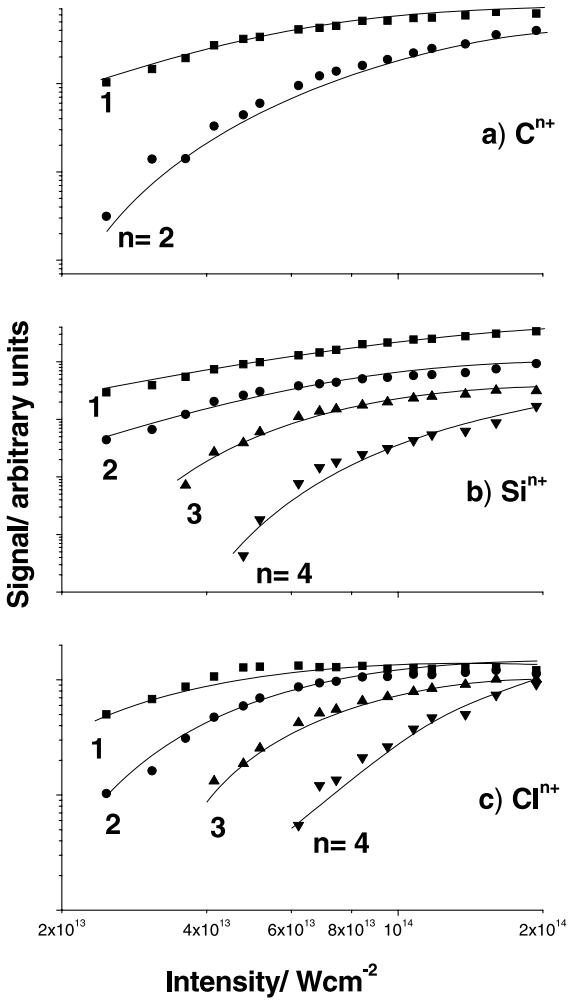

Fig. 5. Dependence with laser intensity of multicharged atomic fragments of 2-chloro-ethenylsilane for the laser wavelength of 800 nm: (a) C ions, (b) Si ions and (c) Cl ions. Lines are drawn to guide the eye.

3.2. Splitting of multiply charged ion peaks

Following interaction with laser pulses at 800 and 400 nm, signals corresponding to multiply charged C, halogen and Si atoms were found to split into two components. The characteristics of the observed peak splitting provide hints about the ionization and dissociation mechanisms [5]. The characteristic doublet structure is exemplified in Fig. 1. The peak profiles exhibit a broad fast component and a narrow slow component. Similar structures have been previously reported [2,6] and have been presented as evidence of a Coulomb explosion event [26]. The splitting reveals the different arrival times for the ions ejected with a range of kinetic energies heading towards the detector, in parallel direction to the laser polarization vector, and ions ejected in the opposite direction (forward and backward with respect to the TOF axis).

The fragment kinetic energy E_{kin} can be obtained from the temporal peak separation, Δt, through the relation $E_{kin} = e^2q^2U^2\Delta t^2/8M$, where e is the elementary charge and U is the collection electric field of the TOF spectrometer, about 1300 V cm^{-1}. A summary of calculated kinetic energies of the ejected muticharged atomic ions is given in Table 1. One can see that ions with higher charge multiplicity are released with faster velocities. Moreover, the relative kinetic energy of the C and halogen fragments is greater for the larger 2-chloro-ethenylsilane system than for chloro- and bromo-ethylene. In the former Si, Cl and C ions are released in increasing order of kinetic energies. We have also observed that the increase of laser

Table 1
Calculated kinetic energy release (in eV) of multicharged atomic cations obtained at 800 nm and 2×10^{14} W cm^{-2}

	$H_2C{=}CHCl$	$H_2C{=}CHBr$	$H_3SiCH{=}CHCl$
C^{2+}	42	49	78
C^{3+}	61	61	198
Cl^{2+}/Br^{2+}	14	10	32
Cl^{3+}/Br^{3+}	29	[a]	131
Cl^{4+}/Br^{4+}	33	30	233
$Si^{2+}/Si^{3+}/Si^{4+}$			26/55/85

[a] Not given for Br^{3+} due to overlap with $C_2H_3^+$.

intensity results in larger kinetic energies for the ejected ions [20].

4. Discussion

The ion distributions measured here reveal the predominance of two different mechanisms at the two laser wavelengths and the influence of the molecular structure in the laser–molecule coupling. Ionization and fragmentation can either proceed through a 'ladder-switching' mechanism or by a direct, instantaneous explosion of the parent molecule [2]. In the ladder switching pathway, some polyatomic fragments originated in the primary ionization step undergo further ionization during the laser pulse if dissociation is fast. Multiphoton ionization (MPI) and field induced (FI) tunnel ionization can contribute to both cases, depending on the laser intensity and wavelength. As the intensity increases the transition between the MPI and FI tunnel ionization regimes occurs according to the value of the adiabaticity parameter [27] $\mathrm{AP} = (E_i/(1.87 \times 10^{-13}\ I_0\lambda^2))^{1/2}$, where E_i is the molecular ionization potential (in eV) in the absence of the laser field, I_0 is the peak laser intensity (in W cm^{-2}) and λ is the laser wavelength (in μm). Values of $\mathrm{AP} > 1$ are indicative of a MPI mechanism, values of $\mathrm{AP} < 1$ imply the participation of an FI mechanism.

A proposed structure-based model [28] predicts that the transition to the FI regime occurs in a molecule at lower laser intensity than that expected for an atomic species of the same ionization potential. The ionization potential of the molecules of this study is around 10 eV [21]; therefore, at the highest laser intensity of the 800 nm pulses (2×10^{14} W cm^{-2}), $\mathrm{AP} \ll 1$. Although FI effects should prevail in the interaction at the maximum laser intensity and longest wavelength, parent monocations can also be formed in the leading edge of the pulse and subsequently multiply ionized. These processes take place at lower intensities and involve species of higher ionization energy, implying substantially larger values of AP. In addition, outside the laser focal zone the laser intensity reaches values that are considerably smaller than its maximum. Hence both MPI and FI are likely to participate in the dissociative ionization processes occurring at 800 nm. However at this wavelength the FI ionization mechanism should be enhanced, accounting for the efficient formation of the parent dication at 800 nm. At 400 nm the characteristic values of AP are much higher and a MPI mechanism should preferentially drive the laser–molecule interaction.

In the MPI picture the number of photons of wavelength of 400 nm required to produce parent dications is half the number required at 800 nm. Laser pulses of 400 nm with the same number of photons as pulses of 800 nm would produce a larger yield of parent dications. This is contrary to our observation, as at the same laser intensity of both wavelengths (i.e., when the number of photons is twice as large at 400 nm) pulses of 400 nm induce fragmentation processes that dominate over the formation of the dication (Figs. 1 and 2). The patterns of dissociation at 400 nm are consistent with the fragmentation channels identified for the neutral molecules [29–31]. This provides support to the idea that different mechanisms should be predominant at each wavelength.

When the laser intensity increases, the parent, and possibly other polyatomic fragments from the primary dissociation step, reach higher stages of ionization leading to Coulomb explosion into atomic multiply charged ions. If the fragmentation favors charge symmetry, then the observation of highly charged atomic fragments (charge multiplicity up to 5) would imply the existence of molecular transients that have twice the atomic charge.

On the other hand the characteristic peak splitting of multiply ionized atomic fragments can be rationalized by invoking the properties of the molecular structure. The higher polarizability of the silane compound allows a higher mobility for the charges driven by the electric field. Consequently it is easier to strip out electrons of this molecule. Moreover, a larger geometrical length facilitates the acceleration of the electron inside the potential energy surface to higher kinetic energies. The obtained kinetic energies are consistent with a Coulomb explosion mechanism occurring in the high intensity spatial region of the laser beam. As the laser intensity increases,

the parent molecule (or the precursor polyatomic fragments) reaches higher stages of ionization that lead to stronger repulsion between fragments and then to higher kinetic energies. Thus, fragments with higher charge multiplicity are ejected at faster velocities. The fact that the kinetic energy release scales with charge multiplicity indicates that multiply charged ions are not produced by subsequent ionization of ions of lower charge but rather by independent processes originating from the parent precursor in various stages of ionization. Moreover, the short duration of the pulse precludes the occurrence of these 'ladder switching' processes in which photoabsorption and dissociation of fragments are repeated sequentially leading to smaller size fragments. According with the results shown above, Coulomb explosion of the silane derivative takes place at lower laser intensities than the corresponding to chloro- and bromo-ethylene.

5. Conclusions

The coupling between intense 50 fs laser pulses of 400 and 800 nm and the molecules of these study has shown to depend on both the wavelength of the laser and on the molecular structure. At 400 MPI processes dominate the interaction and result in efficient fragmentation of the parent ion in consistency with the fragmentation channels of the neutral systems. At 800 nm fragmentation is reduced as evinced by the higher yield of parent singly and doubly charged cations and the presence of intense peaks attributed to multicharged atomic constituents. Peak splitting of the latter provides a signature of Coulomb explosion taking place at the high intensity regions of the laser pulse. The stability of the multicharged parent ion decreases as the molecular size increases. The Coulomb explosion event takes place at lower intensities in the silane derivative and results in more energetic multicharged atomic fragments. The data also reveal an efficient energy coupling between the laser and the nuclear modes that increases with molecular size. This points out to the existence of truly collective molecular effect as opposed to the coupling to a collection of independent atom and indicates that the interaction takes place with the molecular structure as a whole.

Acknowledgements

The experiments were performed at the Ultraviolet Laser Facility, FoRTH-IESL thanks to financial support provided by the Large Installations Plan of EU. This research has benefited from support of Project BQU2000-1163-CO2-01 (DGI, MCyT, Spain). M.C. is grateful for the hospitality received as a Visiting Scholar at the Chemical Laboratories, Harvard University.

References

[1] A.N. Markevitch, N.P. Moore, R.J. Levis, Chem. Phys. 267 (2001) 131.
[2] P. Tzallas, C. Kosmidis, K.W.D. Ledingfham, R.P. Singhal, T. McCanny, P. Graham, S.M. Hankin, P.F. Taday, A.J. Langley, J. Phys. Chem. A 105 (2001) 529.
[3] A. Talebpour, A.D. Bandrauk, K. Vijayalaksmi, S.L. Chin, J. Phys. B 33 (2000) 4615.
[4] S.M. Hankin, D.M. Villeneuve, P.B. Corkum, D.M. Rayner, Phys. Rev. Lett. 84 (2000) 5082.
[5] S. Banergee, G.R. Kumar, D. Mathur, J. Phys. B 32 (1999) 4277.
[6] S. Shimizu, J. Kou, S. Kawato, K. Shimizu, S. Sakabe, N. Nakashima, Chem. Phys. Lett. 317 (2000) 609.
[7] M. Castillejo, S. Couris, E. Koudoumas, M. Martín, Chem. Phys. Lett. 289 (1998) 303.
[8] M. Castillejo, S. Couris, E. Koudoumas, M. Martín, Chem. Phys. Lett. 308 (1999) 373.
[9] J.H. Phostumus, J. Plumridge, M.K. Thomas, K. Codling, L.J. Frasinski, A.J. Langley, P.F. Taday, J. Phys. B 31 (1998) L553.
[10] S. Couris, E. Koudoumas, S. Leach, C. Fotakis, J. Phys. B 32 (1999) L439.
[11] D. Normand, L.A. Lompré, C. Cornaggia, J. Phys. B 25 (1992) L497.
[12] B. Friedrich, D. Herschbach, Phys. Rev. Lett. 74 (1995) 4623.
[13] J.J. Larsen, H. Sakai, C.P. Safvan, I. Wendt-Larsen, H. Stapelfeldt, J. Chem. Phys. 111 (1999) 7774.
[14] N. Hay, M. Castillejo, R. de Nalda, E. Springate, K.J. Mendham, J.P. Marangos, Phys. Rev. A 61 (2000) 53810.
[15] N. Hay, R. de Nalda, T. Halfmann, K.J. Mendham, M.B. Mason, M. Castillejo, J.P. Marangos, Phys. Rev. A 62 (2000), 041803-1.
[16] H. Rabittz, R. Vivie-Riedle, M. Motzkus, K. Kompa, Science 288 (2000) 824.

[17] C. Cornaggia, D. Normand, J. Morellec, J. Phys. B 25 (1992) L415.
[18] A. Talebpour, S. Larochelle, S.L. Chin, J. Phys. B 31 (1998) 2769.
[19] M. Lezius, V. Blanchet, D.M. Rayner, D.M. Villeneuve, A. Stolow, M.Y. Ivanov, Phys. Rev. Lett. 86 (2001) 51.
[20] M. Castillejo, S. Couris, E. Koudoumas, R. de Nalda, M. Martin, J. Phys. Chem. A, in press.
[21] Handbook of Chemistry and Physics, CRC Press, Boca Raton, FL, 1999.
[22] A.E. Siegman, Lasers, University Science Books, Mill Valley, CA, 1986.
[23] P. Hansch, M.A. Walker, L.D. Van Woerkom, Phys. Rev. A 54 (1996) R2559.
[24] A. Talebpour, C.Y. Chien, S.L. Chin, J. Phys. B 29 (1996) L677.
[25] J. Pola, Z. Bastl, J. Subrt, J.R. Abeysinghe, R. Taylor, J. Mater. Chem. 6 (1996) 155.
[26] P. Hering, C. Cornaggia, Phys. Rev. A 59 (1999) 2836.
[27] L.V. Keldysh, Sov. Phys. JETP 20 (1965) 1307.
[28] R.J. Levis, M.J. DeWitt, J. Phys. Chem. A 103 (1999) 6493.
[29] D.A. Blank, W. Sun, A.G. Suits, Y.T. Lee, S.W. North, G.E. Hall, J. Chem. Phys. 108 (1998) 5414.
[30] R.D. Kay, L.M. Raff, J. Phys. Chem. A 101 (1997) 1007.
[31] M. Castillejo, R. de Nalda, M. Oujja, J. Photochem. Photobiol. A 110 (1997) 107.